IAC-12-A6,P,15

COLLISION PROBABILITY ASSESSMENT FOR ACTIVE DEBRIS REMOVAL MISSIONS

Aleksander Lidtke
University of Southampton, United Kingdom, al11g09@soton.ac.uk
Hugh G. Lewis
University of Southampton, United Kingdom, H.G.Lewis@soton.ac.uk

Increasingly larger investments are being made world-wide in the technologies necessary to perform Active Debris Removal (ADR) due to a growing concern about the sustainability of spaceflight. In-orbit validation of certain concepts appears likely in the near future with potential implementations to follow shortly afterwards. Little to no attention appears to be given to the risks associated with such missions, however, which raises concerns about the impact of the ADR missions themselves. This study conducts an assessment of the probability of an in-orbit collision occurring between an ADR mission's target, whilst being de-orbited, and all the objects in the public catalogue published by USSTRATCOM. Such a collision could have disastrous effects as the target is most likely going to be located in densely populated orbital regimes and thus many follow-up collisions could take place. Two impulsive and one low-thrust example ADR mission trajectories that can be associated with particular types of de-orbiting technologies are screened for conjunctions. The importance of extremely close conjunctions that result in most of the total accumulated collision probability (in excess of 99% in certain cases) and the need to avoid those is highlighted. This likely discards ADR technologies that do not enable collision avoidance to be performed. Collision avoidance during debris removal appears of particular importance if business is to be built around ADR in order not to undermine the credibility of the ADR companies if they were to cause catastrophic collisions. It is also suggested that, depending on the removal method, it may be less risky to the debris environment to leave the target object in orbit for longer and perform fewer removals per year but with a lower probability of collision.

I INTRODUCTION

Active Debris Removal (ADR) is believed to be necessary in order to preserve mankind's access to the vital resource of Space. Considerable investments are being made world-wide in the development of necessary technologies and in-orbit validations are likely to materialise in the near future.

Rendezvous and interaction with an uncooperative and unprepared object has never been done before and, as such, is going to be highly challenging. Many vastly different concepts for ADR technologies are being proposed and significant research is being done in order to try and reduce the tremendous cost of removing as many objects as believed necessary to halt the increase of the number of debris.

However little to no attention is being given to the risks associated with performing ADR. Recent studies at the University of Southampton have shown that failures of ADR missions may have a detrimental effect on the debris environment. But the most severe outcome of an ADR mission failing would be a catastrophic collision that would not only offset the benefit of such an initiative but also undermine the support for it.

This research aims to address this issue and assesses various proposed ADR architectures' probabilities of causing a collision in orbit. It is expected that certain approaches will be more prone to this than others, potentially to an extent that would make this architecture selection criterion as important as e.g. the total mission cost. This primarily applies to the types of mission orbits used but these often imply specific technology sets.

First, the method of detecting conjunctions and assessing them in terms of collision probabilities will be developed. Then three example ADR trajectories that correspond to vastly different architectures will be put forward and screened for conjunctions against the public two-line element catalogue. Their collision probabilities will be compared to one another and their target, if it were to be left in orbit, and conclusions will be drawn hence.

II METHODOLOGY

This section describes the methods that have been used to quantify collision probabilities of example Active Debris Removal mission architectures. First an algorithm that enables conjunctions to be identified is described. Next the process for calculating the collision probability of every such an event is given. Finally a brief validation is presented.

II.I Conjunction Detection

A conjunction has been defined as a time interval when two objects' centres of mass are within a certain distance threshold from one another. Ellipsoidal threat volumes can also be used for conjunction screenings in order to tackle the position uncertainties that are not the same in every direction, but it was decided to account for this when computing the collision probability for every conjunction[1,2]. Furthermore, conjunctions between more than two objects have been treated as multiple conjunctions of pairs of objects.

Even with such a simple formulation of a conjunction the computational time required to identify them between a target object and all of the objects in the public catalogue (approx. 15 000 objects as of October 2013[3]) is significant. This raises the need to implement a number of so-called pre-filters that discard pairs of objects that cannot have a conjunction based on simple and fast to evaluate flight dynamics principles.

The entire simulation period was split into time intervals in which all the object pair combinations were analysed. The Cartesian position, velocity, and orbital elements of the objects at the beginning of every analysis interval were used to pre-filter the objects. If all the pre-filters were passed the minimum distance between the objects in this analysis interval would be found together with the corresponding time of closest approach (TCA). If the objects got closer than the threshold distance the collision probabilities would be computed and the conjunction recorded. The entire process was repeated in the following analysis intervals until the end of the simulation was reached.

The pre-filters that are utilised in this work will now be described and the scheme used to find the precise times of the closest approach between objects will be described next.

II.I.I Pre-filtering Stage

A number of pre-filters have been developed to date, starting with the work by[4] that is still being used as well as alternative approaches adopted by [5], [6] and [7]. However, some of them are inapplicable to certain types of orbits (e.g. the orbit path filter that is only applicable to non-coplanar orbits[8]) or require the orbit to be provided in a specific format (e.g. mean elements[4]). Therefore only the pre-filters that have been implemented to produce the results discussed herein, which are a modification of the "smart sieve" pre-filter set[6], will be presented for brevity. The filters will be described in the same order as they are implemented in the simulation code.

Every object in orbit can be associated with an altitude band where it resides, even if it does not follow an orbit that can be approximated as Keplerian. This forms the foundation on which the first pre-filter, the perigee-apogee filter, works[4]. Because of its generality and the fact that this pre-filter does not produce false negatives[6] the perigee-apogee filter has been implemented in this work but with a contingency of 50 km. This is to say that the difference between the perigee and apogee altitudes of the two objects at every analysis time step would need to be higher than the conjunction threshold distance plus 50 km in order for the pair not to be further analysed in this time interval. However, if the difference were 1000 km or more the pair would be discarded from further analysis in all the remaining intervals as the two objects would clearly not cross each other's altitude bands unless manoeuvres were performed and this study has only looked at much smaller overall altitude changes (at most 250 km throughout the entire mission). This 1000 km threshold was not originally implemented in the "smart sieve"[6].

Another pre-filter that makes no assumptions as to the trajectories of the objects of interest, the X, Y, Z sieve, was developed by [5] and was also implemented by [6]. This is because it is only concerned with the components of the Cartesian positions of the objects at any given time. This filter uses an observation that if any Cartesian coordinate pair of two objects at the beginning of a given analysis interval varies by more than a certain screening threshold, c, here adopted from the "smart sieve", there is no chance that they could have a conjunction. For example, a potential conjunction pair, i and j, will be rejected using the z coordinate if

$$\left|z_i - z_j\right| > c. \quad [1]$$

Limiting the problem to Earth-satellites allows further simplifications, firstly by observing that no objects can move with respect to each other faster than twice the surface escape velocity at any time[6]. If the analysis interval is known, a distance, R_{th}, referred to as the threshold radius in [6], may be defined:

$$R_{th} = R_{conjunction} + v_{escape} \times \Delta T \quad [2]$$

If the distance between the two objects at the beginning of the analysis time step, ΔT, is greater than this threshold value the two objects cannot get within the conjunction distance threshold ($R_{conjunction}$) during this analysis interval[6]. Furthermore, if a given object pair is separated by more than R_{th} in the given time interval, a number of subsequent intervals may be skipped[6] as

$$N_{skip} = int\left(\frac{r - R_{th}}{2}\right), \quad [3]$$

where r is the actual separation distance between the objects at the beginning of the analysis time step and int denotes the integer part of a number.

Equation [2] does not account for the effects of gravity, i.e. it assumes linear relative motion. The maximum acceleration between a given pair of objects can never exceed twice the surface value, g_0[6]. Hence, a maximum distance, R_{acc}, can be established that ensures that the secondary object, if it does get within $R_{conjunction}$ from the primary in the current analysis time step, will be picked up in the same fashion as with the threshold radius but accounting for the acceleration effects:

$$R_{acc} = R_{conjunction} + g_0 \times \Delta T^2. \quad [4]$$

All the above pre-filters have been adopted from (6) but during testing it was discovered that the "smart sieve" steps that use the threshold radius given in equation [2] occasionally produce false negatives. However, when a contingency factor of 2.0 was used,

i.e. when twice the threshold radius was used instead, no false negatives were present for all the tested orbital regimes. This was the only additional modification that has been made to the classical "smart sieve".

II.I.II Range-based Detection

If all the pre-filter stages were passed the time of the closest approach would be computed by finding the epoch when the relative range-rate was zero. Even though a freeware implementation of the simplified general perturbations (SGP4) propagator[9] was used to generate the ephemerides of the secondaries, i.e. not the ADR mission target in question, the simulation framework has been designed to accept any ephemerides' sources. Being able to cope with externally-generated ephemeris tables was of primary importance as it allows high-fidelity propagators to be used with the same framework.

In order to keep the simulation framework insensitive to the ephemeris source an ephemeris table is generated using SGP4 and only the states propagated to the analysis interval epochs are used. These states are interpolated using a piecewise cubic polynomial expressed in a dimensionless time domain in order to avoid singularities. This ensures that the velocity and position are continuous between the neighbouring intervals and limits the number of floating point operations that need to be performed in order to generate the interpolating polynomials.

Furthermore this interpolation scheme allows the relative range, range rate $v(t_k)$, and acceleration $a(t_k)$ between the two objects to be analytically expressed as 6th, 5th, and 4th order polynomials, respectively. This enables the epoch of the closest approach to be found using a simple Newton-Rhapson search[10] to find the point where the relative range rate (square of the range rate is used here to provide computational time saving) is zero. The Newton-Rhapson search is initialised in the middle of the interpolation interval and performed in the following manner[6]:

$$t_{k+1} = t_k - \frac{v(t_k)}{a(t_k)}, \qquad [5]$$

where k is the index of current iteration in finding the root of the relative range rate squared. The number of iterations was limited to 1000 and the TCA convergence criterion to 10^{-8} of the time step (which corresponds to 6×10^{-6} seconds for the nominal time step duration of 600 seconds). The root finding is, as conventionally adopted, terminated when the desired accuracy has been reached or when the maximum number of iterations has elapsed[10].

When the relative range rate is zero a check on the second derivative, i.e. the relative acceleration, should be performed to ensure that a minimum was found rather than a maximum. However, if a maximum were found the relative distance at the TCA would be greater than the conjunction threshold so a range, rather than a second derivative, check can be performed to verify what type of local extreme was found. Normally if roots of the relative range-rate are real, which they will be when using the numerical scheme described herein, they will correspond to minima of the relative range[1].

The analysis interval's duration of 600 seconds was chosen as the computational speed of the entire framework was the greatest with such a step (it is expected for such algorithms to have an optimum time step[6]) and no very close conjunctions were missed. Specifically, the interpolation scheme was accurate to within 20 km (infinity-norm) for all the investigated orbit types. Hence setting the conjunction threshold distance to 20 km guaranteed that no very close conjunctions, which could potentially have extremely high collision probabilities, would be missed. Note that SGP4 accuracy decay was not accounted for here as finding all the conjunctions that would occur in the real world was not the goal of this study.

II.II Collision Probability Estimation

This study is primarily concerned with the inherent risk of all the ADR missions. A method to establish the covariance matrices for this purpose is given first. How these are then converted into collision probability metrics will be described next. Finally an assumption regarding the physical size of the objects, which is important for collision probability calculations, will be investigated.

II.II.I Covariance Matrices

Assuming performance of a Space Surveillance and Tracking system provides an estimate of the risk experienced by any space mission, including ADR.

The European Space Agency has defined an accuracy envelope the European Space Surveillance System (ESSS) shall provide[11,12]. If the system is built according to these requirements, the position of all the objects in orbit shall be known with accuracy no worse than 40, 200, and 100 m in the radial, along-track and cross-track reference frame in the Low Earth orbit (LEO) regime at all times[12]. These standard deviations can readily be used to construct covariance matrices from which the collision probability can be computed.

Since ESSS will catalogue the LEO objects with the said accuracy at any time propagation of the covariance is not necessary as in reality the covariance may only be less. This lower covariance corresponds to smaller uncertainty ellipsoids and hence significantly lower collision probabilities, unless an extremely close conjunction is recorded. The latter case will have a relatively high collision probability.

If an exemplar conjunction geometry is taken and covariance matrices of both objects, denoted as C, are scaled by a constant factor k such that $C' = k^2 C$, the collision probability changes as in Figure 1. It is clear that the smaller the covariance the lower the collision

probability. This will only be true if the miss distance is small compared with the initial standard deviations of position i.e. when the conjunction is not in the probability dilution regime[13]. Even in the dilution region, however, the resulting true collision probability will be lower than the maximum probability.

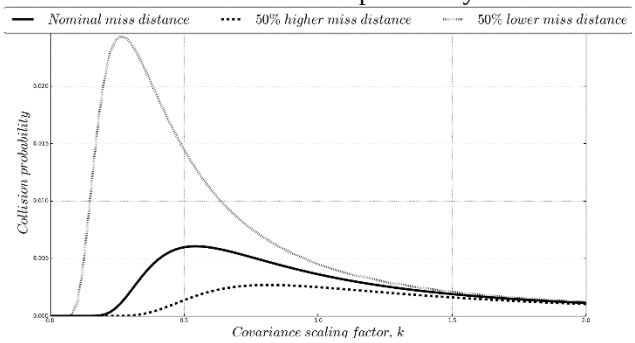

Figure 1: Effects of scaling the combined position covariance matrices by a constant factor k^2 on the collision probability for various miss distances.

It has been decided to compute the maximum collision probability when using the uncertainty ellipsoids' aspect ratios as they would be provided by the ESSS. It was decided that finding the worst-case orientation of the ellipsoids as developed by [13] was not appropriate as it would not reflect the accuracy envelope as given in [12]. The maximum probability computed in this manner provides an approximate upper bound on the collision probability that can be experienced by an ADR mission when the operational decisions are made based on ESSS ephemerides.

The true collision probability was also computed using covariance matrices stemming directly from [12] as that is going to result in the lowest collision probabilities that would be available to support the spacecraft operations.

Such an approach provided two extreme collision probability values and any ADR mission, if its operations were supported by the ESSS, would be placed between these.

The maximum collision probability is found by scaling the covariance matrix C by a constant factor. This scaling factor k can be found analytically by assuming that the probability takes its peak value when the relative position's probability density function (PDF) does (as given in e.g. [14]):

$$k = \sqrt{\frac{p_{mean}^T \, C^{-1} p_{mean}}{2}}, \qquad [6]$$

where p_{mean} is the mean relative position vector of the two objects at the conjunction epoch. This analytical estimate has been found not to be accurate for all the conjunctions therefore a simple golden-ratio search was utilised to find the scaling factor k that gives the actual maximum of the collision probability of every conjunction[10].

II.II.II Collision Probability Estimation

A classical approach, where every conjunction is analysed in a B-plane frame of reference centred on the primary (the ADR mission target) was adopted[14,15,16]. The algorithm steps will now be described in a chronological order, i.e. as they are performed in the simulation.

Position covariances of both objects are rotated to the B-plane according to the algorithm given e.g. by [14], and combined. The velocity covariance is ignored as it has been found not to affect the collision probability significantly[14] and this has been confirmed by Monte Carlo analyses of several exemplar conjunctions. Collinear relative motion is assumed in the vicinity of the TCA thus allowing the covariance matrix to be projected onto the B-plane and reducing the number of dimensions of the problem from three to two[14,16].

The position covariance matrices are then converted into a probability density function and numerically integrated in the Cartesian coordinates of the B-plane (y, z) inside a circle with radius equal to the combined radii of the two objects (collision radius r) and centred on the primary as given in [14,16]:

$$\mathrm{P} = \iint_{z=-r;\, -y=\sqrt{r^2+x^2}}^{z=r;\, y=\sqrt{r^2+x^2}} \frac{2\pi}{\sqrt{\det(C)}} e^{-\frac{1}{2}D^T C^{-1} D} dy\, dz. \qquad [7]$$

In the above equation det denotes the determinant of the matrix and D is the discrepancy vector defined as:

$$D = \begin{bmatrix} y \\ z \end{bmatrix} - p_{mean}, \qquad [8]$$

where y and z are instantaneous values of the free Cartesian in-plane coordinates.

Even though equation [7] can be expressed as an infinite series of analytical terms, thus reducing the time required to compute the collision probability of every conjunction[16], this approach has been found inaccurate in some cases and thus a simple numerical integration scheme[10] was used instead.

Integrating equation [7] yields the probability that both objects' centres of mass will be within the collision radius during the closest approach, i.e. whether a collision will take place. The maximum collision probability can be computed in the same fashion as well if the covariance matrix is scaled beforehand, as mentioned previously.

TLEs come with no information as to the size of the associated objects and thus certain assumptions had to be made in order to enable the collision probability to be computed. These assumptions will be described in the following section.

II.II.III Physical Object Size

A database containing physical radii of objects launched up to 2003 (up to NORAD catalogue number 28057) originally compiled by The Aerospace Corporation was kindly provided by T.S. Kelso[17], thus allowing the collision radius to be computed as accurately as possible for conjunctions involving objects from this database. This implies ignoring the attitude of the objects but this is not expected to change the global trends in collision probabilities as it would only affect the relative importance of individual conjunctions. Such a simplification is therefore acceptable for this study.

For the remainder of the catalogue, the MASTER 2009 population, kindly provided by the ESA Space Debris Office, was analysed and the size of the objects with respect to their type was investigated. An average radius for rocket bodies (R/B), payloads (P/L), mission-related objects (MRO), and debris (DEB) was computed. The standard deviation of every group was also found and the results are shown in Table 1.

Some of the MASTER object types can be directly linked to TLEs through the three-line elements that contain information about the type of certain objects. As the three-line element catalogue does not distinguish mission-related objects, data for this type of object were not directly utilised. Moreover, the three-line element database contains many objects that are not classified as payloads, rocket bodies or debris. For these objects the average size of the entire MASTER 2009 (all four types of objects) population was used.

It was decided that, in the absence of an exhaustive database of object sizes that could associate every Space Surveillance Catalog number (SSC) with a particular object size the statistical values from Table 1 should be assumed whenever an object's size was not available in the database.

Object type	R/B	P/L	MRO	DEB	Other
MASTER Object ID	1	2	3	4	1, 2, 3, and 4
Average radius (m)	1.77	1.77	0.54	0.16	0.35
Standard deviation (m)	0.81	0.78	0.72	0.55	0.78

Table 1: ESA's MASTER 2009 population objects' radii grouped according to the types of objects (rocket bodies (R/B), payloads (P/L), mission-related objects (MRO), and debris (DEB)) also discerned in Space-Track's Three-Line Elements.

Even though the standard deviation for certain types of objects is large it has been found not to affect the overall collision probability by more than approximately 10% when an average MASTER 2009 radius ± one standard deviation is used as long as a database of object sizes is utilised for the remaining objects.

II.III Validation Results

All the conjunctions of Envisat (SSC 27386) closer than 20 km against the entire public TLE catalogue were found. The simulation was performed from the epoch of Envisat's TLE (23 October 2013) until 23 October 2014. The obtained accumulated true and maximum collision probabilities have been compared to the same quantities obtained with Systems Toolkit's Conjunction Analysis Tool (STK CAT). The results are presented in Figure 2.

Due to hardware limitations it was not possible to assign different radii to objects not present in the physical radii's database based on their type. Therefore all the objects not present there were given a radius of 1.0 m.

Furthermore, STK CAT computes the maximum collision probability according to the scheme given in [13] i.e. it finds the worst-case orientation as well as size of the uncertainty ellipsoids. In order to make the developed algorithm compatible with it, unity aspect ratios of the uncertainty ellipsoids had to be assumed.

The achieved errors in the final accumulated true and maximum collision probabilities were 11.6% and 4.2%, respectively. These discrepancies can be attributed to different state vectors and hence also the conjunction geometries returned by the SGP4 propagators used in both cases. These differences can be discerned by noting that the highest maximum probability events, i.e. the ones with the lowest miss distances, occur at different epochs. Even though this would be an issue from an operations point of view it suffices to fulfil the goals of this work.

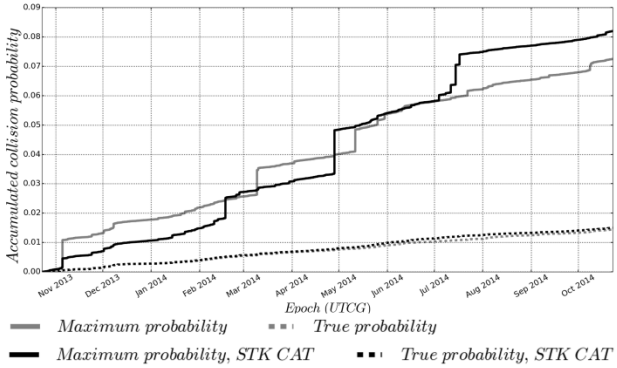

Figure 2: One year of conjunctions of Envisat (SSC 27386) closer than 20 km. Comparison of the accumulated true and maximum collision probabilities obtained with the developed algorithm and System Toolkit's Conjunction Analysis Tool.

III STUDY SETUP

Three example active debris removal architectures have been chosen for this study. These do not represent any particular solutions but have been selected to be different enough to represent as wide a spectrum of potential ADR implementations as possible.

General assumptions, applicable to all the investigated architectures, are given first. Then the assumptions applicable to every architecture individually will be discussed in turn.

III.I General Assumptions

A Zenit-2 rocket body (R/B) has been selected as an example target, as this class of rocket bodies is frequently found to have the potential to take part in catastrophic collisions (18).

Specifically, an object placed in 805 km altitude, near-circular (eccentricity of 0.0011) orbit with inclination of 98.3 degrees was chosen. Its mass, which was used to compute the expected ΔVs, is approximately 9850 kg[18]. The physical radius of the object has been assumed to be 6.377 m according to the data present in the Aerospace Corporation's database for this type of rocket bodies.

No architecture-specific mass or size additions have been investigated as this study has been aimed at investigating general trends exhibited by various groups of concepts rather than specific solutions.

A start epoch of 1st January 2020, 00:00:00.0 UT was chosen, as no full scale ADR mission is expected to be flown beforehand. The starting geocentric, Cartesian position at this initial epoch was $[7183, 0, 0]$ km. This allowed conceptual differences between all the investigated architectures to be clearly visualised as they all started from the same location at the same time.

All phases of the missions that precede the de-orbiting have been ignored as this study was not aimed at investigating various debris capture mechanisms, guidance, navigation and control algorithms and sensors etc.

III.II Architecture-Specific Assumptions

Three example trajectories that can be associated with particular technologies have been chosen for the study. All of them shall now be described in turn.

III.II.I Impulsive

Many ADR solutions that are currently being investigated are based on chemical propulsion and most of them are being designed to remove five objects per year[19,20]. In order to reduce the overall cost of ADR as few launches as possible are sought. This typically results in trajectories that visit many objects rather than dedicated missions to remove individual targets. In order to reduce the amount of fuel on-board, which is also associated with cost, long drift phases are present in such trajectories that rely on the natural gravity perturbations to change the relative right ascension between the ADR vehicle and the target[19].

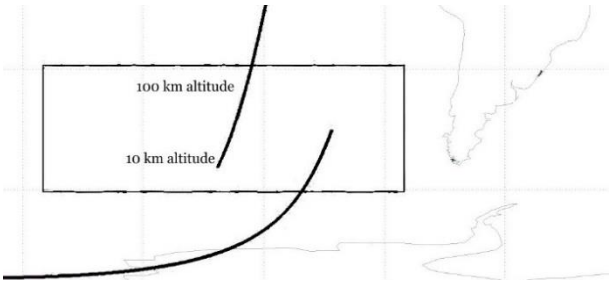

Figure 3: Final revolution of the impulsive trajectory.

The main advantage of chemical propulsion for ADR applications is the capability to target the re-entry into the region of South Pacific Ocean Uninhabited Area (SPOUA) spanning from 29 to 60 degrees south latitude, and 85 to 175 degrees west longitude[21]. This allows the casualty risk on the ground to be reduced and maintained at acceptable levels. It was decided that this targeted re-entry should therefore be included in this trajectory

The initial state vector did not allow a de-orbit manoeuvre to be performed that ensured re-entry over SPOUA close to the initial epoch. Hence a drift of almost 12 days was conducted that ensured that the Zenit-2 R/B's ground track crossed SPOUA close to its centre and an impulsive de-orbit manoeuvre along the orbital velocity direction was conducted then. The epoch and magnitude of the burn were chosen so as to ensure that the entire part of the trajectory below 100 km altitude lied above SPOUA and that the perigee altitude of the last revolution was 0 km[21].

The final revolution of the developed trajectory is shown in Figure 3. This trajectory could be optimised to reduce the total ΔV but this study was aimed at investigating the general trends in the collision probability rather than finding the best possible trajectories, so the optimisation was not performed.

III.II.II Impulsive without Extensive Drift

If a single debris is targeted by an ADR mission sufficient fuel may be available to avoid long coast phases. This will certainly reduce the collision risk while requiring larger active right ascension changes and hence higher overall mission ΔV. This may be desired and intended, however, or spare fuel may simply be available in the spacecraft close to the end of its life.

The trajectory for this architecture is conceptually similar to the previous impulsive one as a positive, targeted de-orbit into SPOUA is performed. But rather than conducting a long drift to wait until the trajectory passes over the target re-entry area an inclination change manoeuvre is performed that takes the spacecraft directly over SPOUA after the first three orbital revolutions. This was performed together with a manoeuvre along the velocity direction that reduced the perigee altitude to 0 km. A part of the ground track of this trajectory is shown in Figure 4.

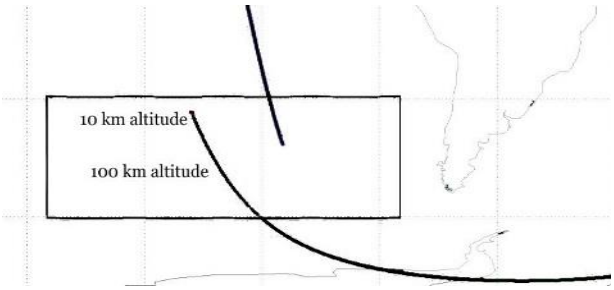

Figure 4: Final revolution of the impulsive trajectory that does not employ natural right ascension drift but uses a manoeuvre to take the trajectory over SPOUA for re-entry.

III.II.III Low-Thrust

A low-thrust trajectory that employs continuous thrust of 25 mN in the anti-velocity direction was also used. This changed the altitude of the Zenit-2 R/B to approximately 550 km. In principle further lowering of the altitude is possible but this altitude ensures re-entry within 25 years from the end of the mission and is thus considered sufficient. Performing a controlled re-entry is desirable but targeting a re-entry area is not possible with low-thrust trajectories.

In the scope of ADR such a trajectory is often proposed with e.g. electrodynamic tethers or drag augmentation devices, not only traditional low-thrust engines. Such deorbiting technologies offer considerable cost savings to ADR in general and are thus often favoured. This is mainly because removal of many objects per year is deemed necessary and lowering the cost of deorbiting individual objects appears to be the only way to make such an approach to ADR economically feasible.

The evolution of the instantaneous radius (computed at 1 day intervals) for the low-thrust trajectory is shown in Figure 5.

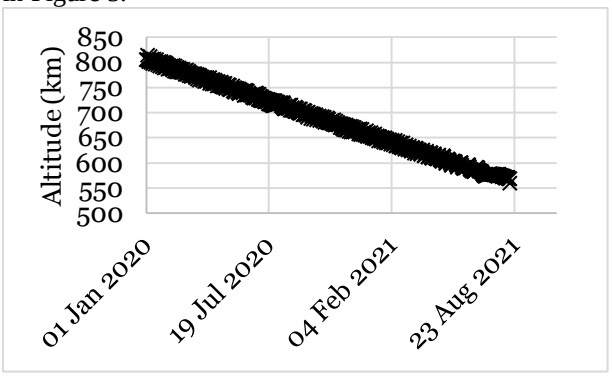

Figure 5: Instantaneous radius of the low-thrust trajectory computed at 1 day intervals.

IV RESULTS

For every of the three trajectories given in section III the conjunctions were found and assessed according to the algorithm outlined in section II.

Specific impulses of 300 and 3400 seconds[22] were also used for chemical and low-thrust propulsion systems, respectively, in order to compute approximate fuel masses for the examined architectures.

Conjunctions involving objects that re-entered before the epoch of the conjunction were filtered out.

The reference accumulated collision probabilities for the Zenit-2 R/B were computed from 23rd October 2013 until 23rd October 2014 using the same covariance, TLE set, objects' physical radii, and algorithms as for the three examined architectures. Such timing ensured that the least error was incurred by the SGP4 propagator as it was the closest to the epochs of most of the TLEs used. A brief comparison of the key figures of merit for every architecture is given in Table 2.

As can be anticipated the longer a mission the higher the collision probability it accumulates as more conjunctions take place.

This general trend can be offset by very close conjunctions, however. It is common for extremely low miss distance conjunctions to have accordingly high collision probabilities. This is especially the case in certain relative geometries that align the uncertainty ellipsoids thus resulting in relatively low combined covariance.

To illustrate this point, 80 out of the total of 14741 conjunctions (0.54% w.r.t. the original value) from the low-thrust trajectory with the highest maximum collision probabilities were filtered out. The final accumulated true and maximum collision probabilities changed to 1.63E-06 and 3.63E-03, respectively. This means that a small fraction of the conjunctions contributed 99.90% and 63.65% to the final accumulated true and maximum collision probabilities, respectively.

It also has to be pointed out that certain architectures have higher maximum collision probabilities than the target left in its original orbit for one year.

V DISCUSION

It has been pointed out that the collision probability of every ADR trajectory investigated is approximately proportional to the duration of the mission. Statistically this is to be expected as all the investigated architectures target the same object and thus operate in the same orbital regimes.

Events that will have much higher collision probabilities than most others throughout the entire mission will occur, however. Such extremely dangerous conjunctions are normally avoided during spacecraft operations by postponing the manoeuvres or even conducting dedicated collision avoidance. Not every proposed ADR architecture provides such control, however. This could result in situations whereby a collision of the object being removed would take place solely because it has been interfered with. It is doubtful, therefore, whether choosing a technology simply

because it is cheaper, thus allowing removal of more object per year, but at an expense of higher collision probability is a sensible choice given the potential to harm, rather than benefit, the debris environment. The only situation where such a technology might prevail is removal of all the uncontrolled objects from orbit.

In fact the collision probability of an object in an altered trajectory can be higher than if no ADR mission is flown to remove it. Behaviour like this is not counterintuitive and precautions ought to be made to avoid causing an orbital collision through ADR. This is not only because an event like this may offset the benefits of performing active debris removal despite considerable investments that will be needed to realise it. Causing a collision while performing ADR would doubtlessly cause debris owners and launching states to be reluctant to allow, let alone fund, further removal of their objects. This might also impact the entity responsible for performing said ADR mission as they would be in control of the object when it took part in the collision[23].

Architecture	**Impulsive**	**Impulsive no-drift**	**Low-thrust**	**Reference Zenit-2 orbit**
Mission duration (days)	11.55	0.13	593.14	365.25
Specific Impulse (sec)	300	300	3400	N/A
Fuel mass (kg)	712.9	2206.9	38.2	N/A
Accumulated maximum collision probability (-)	1.49E-04	3.73E-05	9.94E-03	6.38E-03
Accumulated true collision probability (-)	1.12E-11	1.11E-16	1.56E-03	1.85E-03
Controlled de-orbit (T/F)	1	1	0	0

Table 2: Comparison of the three examined architectures together with reference results for the Zenit-2 R/B in its unaltered orbit.

The fact that an ADR mission may be more risky in the short-term than performing no debris remediation, however, should not be perceived as an argument against it. One can easily imagine that leaving a large number of derelict, uncontrolled objects in orbit for an arbitrarily long period of time is eventually going to results in collisions. It is the exact nature of the removal mission that is in question, not the very idea of performing ADR.

VI CONCLUSIONS

The potential of three different Active Debris Removal architectures to cause orbital collisions whilst attempting to remove an example target object was investigated. Even though primarily trajectories were looked at in this study these can be associated with specific groups of removal technologies.

First of all, it was noticed that ADR may be more prone to causing a collision than leaving the object in orbit for more than a year. This implies that removing fewer objects per year but in a safer manner may be less dangerous to the environment than trying to increase the removal rate at the expense of the collision risk.

This effect will be even more profound if architecture-specific increase in the collision cross-section area is taken into account. For example, long tethers or large solar arrays will make ADR missions even more risky c.f. leaving the target in its orbit for longer.

Secondly, an issue about the liability of the entity performing the ADR was raised. If a business case is to be built around active debris removal, it is in the interest of the ADR companies to ensure that they do not cause orbital collisions as this might cause damage claims but, more importantly, damage the profile of the company.

Finally, the point has been made that most of the accumulated collision risk stems from relatively few very close conjunctions. Even the very improbable conjunctions may cause collisions but our forecasting abilities limit the data that are available to support operational decisions for all spacecraft. Therefore, if extremely dangerous conjunctions are forecast they should be avoided as they are our best estimates of the events that will cause collisions. Hence ADR architectures that do not allow such avoidance actions and ignore the potential risk they introduce should not be considered for implementation.

VII ACKNOWLEDGEMENTS

Authors would like to thank the ESA Space Debris office for allowing them to use the MASTER 2009 population. Dedicated thanks go to Dr Holger Krag and Dr Tim Flohrer for their extremely valuable feedback and help in validating the collision probability algorithms.

Big thanks Dr David Vallado for distribution of the SGP4 propagator code, without which this research would never be possible in the timeframe available.

The authors would also like to express their gratitude to Dr T.S. Kelso for useful comments regarding the collision probability algorithms, maintaining the CelesTrak website, and provision of the objects' physical radii database.

The authors would also like to acknowledge the use of AGI's Systems Toolkit in the verification process of the developed simulation framework.

Most of all, sincere thanks to Dr Claudio Bombardelli for providing an example low-thrust ADR trajectory.

VIII REFERENCES

1. Alfano, S., *Determining Satellite Close Approaches, Part II*. 1994, The Journal of Astronautical Sciences, Vol. 42, pp. 143-152.
2. Coppola, V. Woodburn, J., *Determination of Close Approaches Based on Ellipsoidal Threat Volumes*. 1999, Advances in Astronautical Sciences, Vol. 102, pp. 1013–1024.
3. JFCC SPACE/J3, *Space-Track*. [Online] Scitor. [Cited: 11 August 2014.] https://www.space-track.org/
4. Hoots, F.R., L.L. Crawford, R.L. Roehrich, *An Analytic Method to Determine Future Close Approaches*. 1984, Celestial Mechanics, Vol. 33, pp. 143-158.
5. Healy, L.M., *Close Conjunction Detection on Parallel Computer*. 1995, Journal of Guidance, Control, and Dynamics, Vol. 18, pp. 824-829.
6. Rodriguez, J.R.A. et al, *Collision risk assessment with a 'smart sieve' method*. Noordwijk, The Netherlands: s.n., 2002. Joint ESA-NASA Space-Flight Safety Conference.
7. Khutorovsky, Z.N. et al, *Direct method for the analysis of collision probability of artificial space objects in LEO: techniques, results and applications*. Darmstadt, Germany: s.n., 1993. First European Conference on Space Debris.
8. Woodburn, J. et al, *A description of filters for minimizing the time required for orbital conjunction computation*. Pittsburgh, USA: s.n., 2009. AAS-AIAA Astrodynamics Specialist Conference.
9. Kelso, T.S., *Satellite Tracking Software*. [Online] Celestrak, 22 Jan 2000. [Cited: 26 Apr 2014.] http://www.celestrak.com/software/tskelso-sw.asp.
10. Press, W.H. et al, *Numerical Recipes in C++, Second Edition*. Cambridge, UK: Cambridge University Press, 2002.
11. Krag, H. et al, *The European Space Surveillance System - Required Performance and Design Concepts*. Maui, Hawaii, USA: s.n., 2010. 8th US/Russian Space Surveillance Workshop.
12. ESA/ESOC Space Debris Office. *Space Surveillance and Tracking System Requirements Document*. Darmstadt, Germany: ESA/ESOC, 2013. SST-SRD-4434.
13. Alsano, S., *Relating Position Uncertainty to Maximum Conjunction Probability*. s.l.: The Journal of the Astronautical Sciences, 2005, Vol. 53.
14. Berend, N., *Estimation of the probability of collision between two catalogued orbiting objects*. 1, 1999, Advances in Space Research, Vol. 23, pp. 243-247.
15. Alfano, S. *Review of Conjunction Probability Methods for Short-term Encounters*. Colorado Springs, CO, USA: American Institute of Aeronautics and Astronautics, 2006.
16. Chan, K. *International Space Station Collision Probability*. Chantilly, VA, USA: The Aerospace Corporation, 2009.
17. Kelso, T.S. *Personal communication*. 2 December 2013.
18. Bombardelli, C. *Personal communication*. 25 July 2014.
19. Cerf, M., *Multiple Space Debris Collecting Mission—Debris Selection and Trajectory Optimization*. Journal of Optimization Theory and Applications, 2013, Vol. 156. 322879826.
20. Pasa, N. et al, *Target selection and comparison of mission design for space debris removal by DLR's advanced study group*. September-October 2014, s.l.: Acta Astronautica, 2014, Vol. 102. ISSN 0094-5765.
21. S. Martinez et al, *High Reactivity Maneuver Design in ATV Missions*. MD, USA: John Hopkins Applied Physics Laboratory, 2014.
22. Larson, W.J., J.R. Wertz. *Space Mission Analysis And Design, Third Edition*. El Segundo, CA, USA: Space Technology Library, 1999. ISBN 1-881883-10-8.
23. Soucek, A., *Active Debris Removal and questions of export control*. Paris, France: 3rd European Workshop of Space Debris Modelling and Remediation, CNES, 2014.
24. Flohrer, T. *Persona communication*. 3 June 2014.
25. Flohrer, T. et al, *Operational Collision Avoidance for LEO Satellites at ESA*. Okinawa, Japan: s.n. 2011. Proceedings of the 28th International Symposium on Space Technology and Science (ISTS).
26. Floherer, T. et al, *ESA's process for the identification and assessment of high-risk conjunction events*. 44, 2009, Advances in Space Research, pp. 355-363.
27. Domınguez-Gonzalez, R., N. Sanchez-Ortiz. *Classification of TLE-catalogue objects in regard to their long-term collision probabilities*. Paris, France: 3rd European Workshop of Space Debris Modelling and Remediation, CNES, 2014.
28. Kessler, D.J. 1, s.l.: Icarus, 1981, Vol. 48.